# EFFECT OF SHELL CORRECTION ON THE DECAY PATTERN AND HALF LIFE TIMES FOR SPONTANEOUS FISSION WITHIN THE COLLECTIVE CLUSTERIZATION APPROACH

*A dissertation Submitted*

*In Partial Fulfillment of the Requirements for the award of degree of*

**MASTER OF SCIENCE**

**IN**

**PHYSICS**


*Submitted by*

**SHIVANGI BHATIA**

**(ROLL NO. 301704030)**

*Under the Supervision of*

**Dr. Raj Kumar**

*Assistant Professor*



*School of Physics and Material Science (SPMS)*
*Thapar Institute of Engineering and Technology, Patiala-147004*

*June-2019*

*Dedicated to*

*My Father Mr. Baldev Raj Bhatia*

*And My Mother Reeta Bhatia.*

## *Certificate*

I hereby certify that the work presented in this thesis entitled "Effect of shell correction on the decay pattern and half life times for spontaneous fission within the collective clusterization approach" submitted in partial fulfillment of the requirements for the award of degree of Master of Science in Physics at School of Physics and Materials Science, Thapar Institute of Engineering and Technology, Patiala is an authentic record of my own work carried out under the supervision of Dr. Raj Kumar. The matter submitted via this thesis report has not been submitted for the award of any other degree to the best of our knowledge. Work of other authors cited in this dissertation has been duly acknowledged under reference section of this thesis.

**Shivangi Bhatia**

**Date:** 17-Jun-19

This is to certify that the above statement made by the candidate is correct and true to the best of my knowledge.

**Dr. Raj Kumar**

*Assistant Professor*

Thapar Institute of Engineering and Technology

Patiala-147004

## *Acknowledgment*

I would like to express my deep and sincere gratitude to my research supervisor **Dr. Raj Kumar** Assistant Professor, SPMS, Thapar Institute of Engineering and Technology for giving me the opportunity to do my thesis under his invaluable guidance. His dynamism, vision, sincerity and motivation have deeply inspired me. He has taught me the methodology to carry out the research and to present the research works as clearly as possible. It was a great privilege and honor to work under his supervision. The knowledge and skills that he has shared is something that I will never forget.

I am thankful to **Ms. Navjot Kaur Virk,** research scholar, for helping me throughout the thesis patiently. I would also like to thank her for her friendship, empathy, and great sense of humor. Her scholarly advice and scientific approach has helped me in completing my thesis with ease.

I would also like appreciate Prof. **Dr. Manoj K Sharma** and **Dr. Sunil Devi** of SPMS for helping me in understanding the fundaments of nuclear physics.

I am extremely grateful to my parents for their love, prayers, care and sacrifices for educating and preparing me for my future. Also I express thanks to my younger brother Akshay Bhatia who keep motivating me with his cheerful words. His care and love helped me a lot in completion of my research.

My deep gratitude to my friend Gaurav Harjai who selflessly encouraged me to explore new directions in life. His constant support and availability helped me a lot in completing my thesis. My thanks to Manpreet Kaur Puar to always listen to the ideas popped up in my mind regarding thesis work. She has always been a helping hand to me during the journey.

**Shivangi Bhatia**

**Date:** 17-Jun-19

## *Abstract*

In this thesis, the role of shell corrections (δU) on the decay pattern and half life time of various parent nuclei particularly from $^{232}$U to $^{264}$Hs undergoing spontaneous fission in the ground state (T=0 MeV) has been analyzed using the Preformed Cluster-decay Model (PCM) which employs Collective Clusterization Approach of Quantum Mechanical Fragmentation Theory (QMFT) as its main tool. In this thesis, we have extended the work in which the spontaneous fission half life times were fitted using the neck-length parameter (ΔR) in the presence of shell correction energy δU. In present work, half life times excluding the shell correction energy are computed using same neck length. The effects of shell correction energy on the fragmentation potential, preformation probability and minimized charges of the fragments for the decay of various parent nuclei $^{232}$U to $^{264}$Hs are also analyzed.

The thesis comprises of following three chapters:

* Chapter 1: This chapter contains the basic introduction about the nuclear physics, its applications. The radioactive nature of nuclei and nuclear models has also been discussed in details along with an overview to shell corrections and work done so far.

* Chapter 2: The methodology of Preformed Cluster-decay Model is given in detailed manner. All the parameters which are employed to calculate the half life times of parent nuclei have been elaborated.

* Chapter 3: The outcomes of switching off the shell corrections on various parameters like preformation probability, fragmentation potentials that are employed to calculate half life time of the clusters which are preborn in the parent nuclei, are discussed in details. The half life times calculated with and without shell corrections are compared. The effects due to non inclusion of shell corrections on the magicity and atomic number of decaying fragments have also been commented on.

## *Table of Contents*

## *List of Figures*

## *List of Tables*

# *Chapter 1*

# *Introduction*

## 1.1 General

Nuclear physics, as the name itself suggests is the detailed study of nucleus i.e. the nucleons present in it and various forces acting due to the interactions between them. Many scientists have given their contribution in the enhancement of nuclear physics from the earlier 20th century till now. But the most fundamental, beneficial and productive discovery was contributed by *Ernest Rutherford* in 1906, which defines that a highly dense nucleus constitutes the central part of an atom and most of the mass of atom is concentrated in the nucleus [1-2]. The nucleus consists of positive heavy charged particles and electrons which are present to balance the positive charge. No one knew nucleus during this epoch. In 1932, *James Chadwick* discovered that there is a neutral particle as well in the nucleus which was called the neutron. Due to the discovery of neutron, scientists were able to calculate the binding energy of the nucleus. So many theoretical and experimental works have been done in last century after the discovery of neutron explaining various phenomenon in different subfields of nuclear physics. A nucleus must be treated quantum mechanically to describe the internal motion and structure of the nucleus. The inclusion of quantum mechanics and its various aspects lead to building block of many researches in nuclear physics. Quantum mechanics enabled us to unlock various microscopic properties of a nucleus and how those properties can be employed in macroscopic world or in the applications of nuclear physics. Various scientists like Pauli, Dirac, De Broglie used Rutherford model of an atom in elucidating various mechanisms in the nuclear physics.

The broadening of field of nuclear physics led to the development of other fields like particle physics which was developed when particles were accelerated at high energies in order to test the fundamental blocks of matter. The nuclear physics has major contribution in astrophysics as well. Nuclear reaction takes place in the stars continuously and hence nuclear physics helps us in understanding the basic structure of the stars. By the basic understanding of nuclear and atomic physics we get to know about various astrophysical phenomenon.

Nuclear physics holds a wide variety of applications. Most of the developments in energy, medicine, materials etc. originate from the nuclear physics [3-4]. Some are followed below:

- Nuclear physics principles have provided so many therapy methods which help in treatment of cancer, processing nuclear medicines (radioactive tracers) can detect Alzheimer disease, artery disease. X-ray, Positron Emission Tomography (PET), Magnetic Resonance Imaging (MRI) has helped us to sneak inside the body and detect the problem. All these techniques work under the principles of nuclear physics.
- Detection of particles like beta, gamma, and neutrons with the various detectors like scintillation detector, GM counters etc.
- Energy liberated in nuclear fission (in nuclear reactors) can be employed to produce electricity in nuclear power plants. Most of the nuclear power is contributed by nuclear reactors.
- Carbon dating method based on radioactive decay helps archaeologists to understand the origin of artifacts.
- Controlled gamma radiation helps in improving the quality of food by killing pathogenic germs and insects.
- Nuclear batteries are used in space navigation. The energy produced by Plutonium-238 which is provided with robotic feeding is used to carry unmanned flights from earth to the celestial planets.
- Nuclear weapons or bombs are made using nuclear technologies which can be used as a powerful tool in case of war between the countries. Though it must be avoided in any case as results can be devastating.
- Age of different stars can be calculated on the basis of their masses, temperature and their composition and what changes they witness with time.

## 1.2 Stable and Unstable Nuclei

A nucleus is called stable if it possesses equal number of neutrons and protons i.e. N/Z ratio should be equivalent to 1 or nearly 1. Stable nuclei lie on the valley of stability having very high binding energies. As we approach heavy nuclei, Z is higher and hence more neutrons should be added to counter the repulsive Coulomb force between the protons. When more number of protons and neutrons are added, the nuclei proceed away from beta- stability line. The nuclei

distant away from beta-stability line are unstable, having very less binding energies. Every nuclei approach stability by emitting out beta particles (beta-decay process), alpha particles, fragments, neutrons etc. Nuclei far from stability do not require extra push from outside to expel out particles and achieve stability. The process is spontaneous. These nuclei which are far off stability are known as radioactive nuclei. The internal excitation energy of radioactive nuclei is high enough to tear the nucleus apart and convert into fragments.

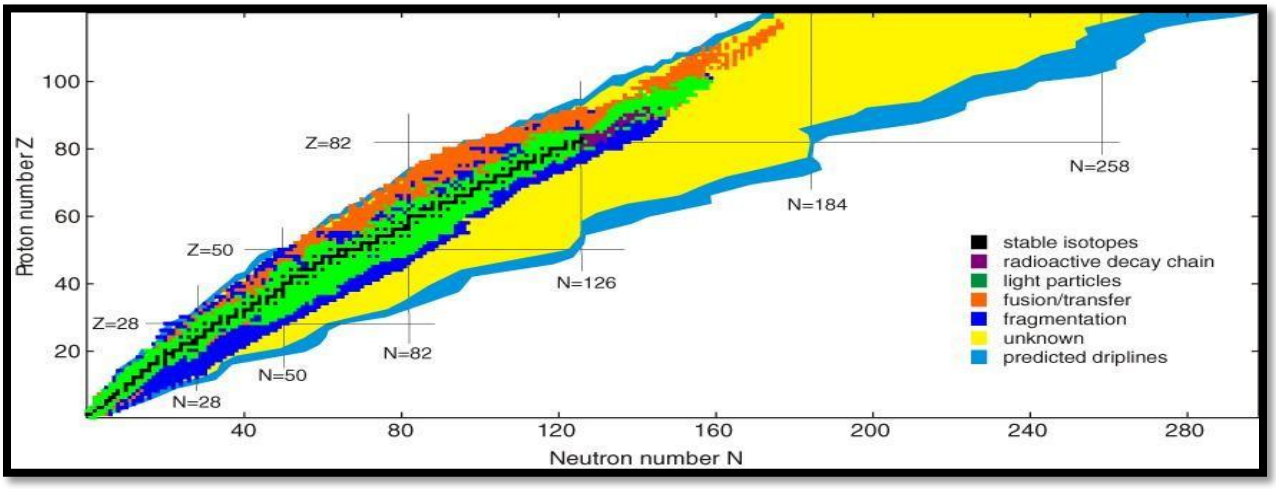


**Figure 1.1** The plot between proton number Z and neutron Number N, known as Segrè plot.

Figure 1.1 depicts the nuclei present on the valley of stability have neutron to proton ratio as 1:1. As the proton and neutron number increases, the nuclei move away from the beta- stability line and starts undergoing various decay processes spontaneous fission, beta decay, alpha decay etc. due to instability.

## 1.3 Radioactivity

An excited state nucleus (unstable) gives out its extra energy and comes down to the ground state (stable state) by ejecting out alpha particles or daughter fragments (heavier than the alpha particles) *i.e.* the clusters. There is ejection of neutrons, gamma rays, beta particles as well in some cases. Common examples of radioactive nuclei are Thorium, Uranium etc. The characteristic of radioactive nuclei is primarily governed by their half life ($T_{1/2}$) or decay constant ($\lambda$). The three major kinds of radioactive processes are as follows:

* **Cluster Radioactivity:** A decay in which a cluster of small number of neutrons and protons is emitted with another daughter fragment. The size of cluster emitted is more

than the size of an alpha particle but less than the size of typical daughter fragment. This is generally seen in nuclei having Z>40.

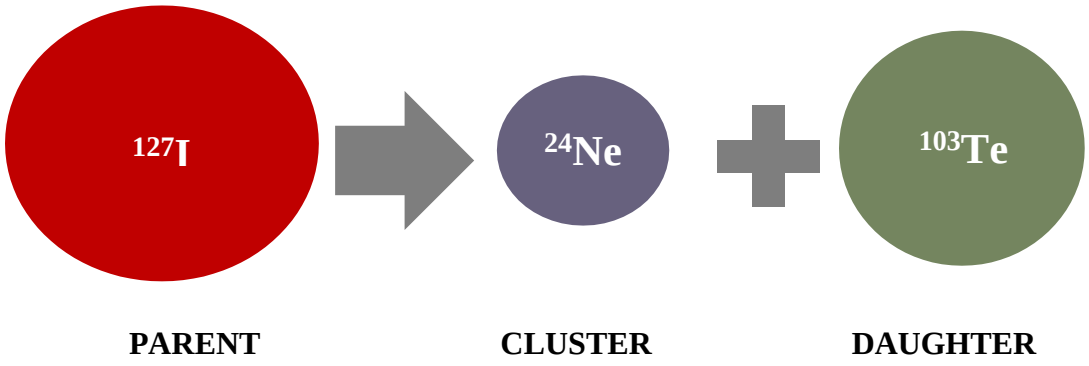


**Figure 1.2** Parent nuclei decays into a cluster and a daughter.

Figure 1.2 depicts the cluster decay process. $^{127}$I being the radioactive nucleus decays into a cluster $^{24}$Ne and a daughter $^{103}$Te. The size of cluster is much less in comparison with the mass of daughter fragment.

* **α-radioactivity:** When a radioactive parent nuclei expels out an α particle as one of its daughter fragment is called α-radioactivity. It is seen in heavy nuclides having atomic number greater than 28(Nickel). A nuclei having large size and so many protons inside it witnesses strong electromagnetic repulsion which can't be counterbalanced by the nuclear force as it is short range. Hence, alpha particle expels out to increase the stability of the parent nuclei by decreasing its size.

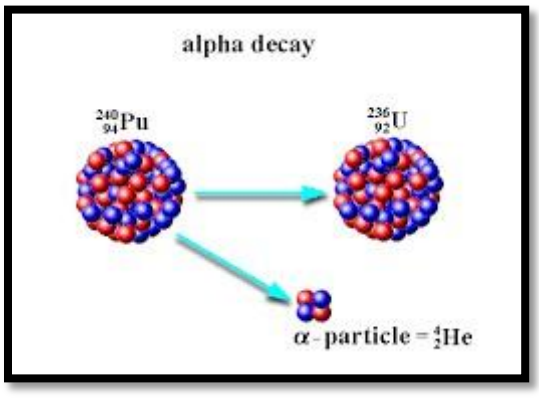


**Figure 1.3** α-decay process of $^{240}$Pu.

Figure 3 depicts a Plutonium nucleus $^{240}Pu$ being large in size and having so many protons (94) ejects out an alpha particle and $^{236}U$ nucleus.

* **Spontaneous Fission:** In Spontaneous fission as the name suggests, the reaction mechanism is spontaneous i.e. it is the radioactive decay which corresponds to division of parent nucleus (heavier) into its daughter components without supplying energy from outside.

This process can proceed in two ways, either the excitation energy of parent nucleus is sufficient to overpower the effect of Coulomb barrier but if the excitation energy of parent nucleus is not adequate enough to undergo radioactive decay then the daughter nuclei undergo quantum tunneling which means it will knock the surface of the parent nucleus repeatedly with certain frequency to come out of the parent nucleus.

In heavy elements from Thorium onwards, the probability of spontaneous fission increases. The probability increases with atomic number of radionuclide.

* One can determine the half lives of radionuclide. For e.g. $^{252}Cf$ has the half life of 2.6 years, decays by α-emission with 96.91% probability and the other half decays having probability of 3.09%.
* The average number of neutrons can be determined that are emitted in the process. For e.g.: 3.7 neutrons on an average are emitted in the spontaneous fission of $^{252}Cf$.
* Rate of fission can be calculated during the decay process.
* Average size of emitted daughter nuclei can be predicted.

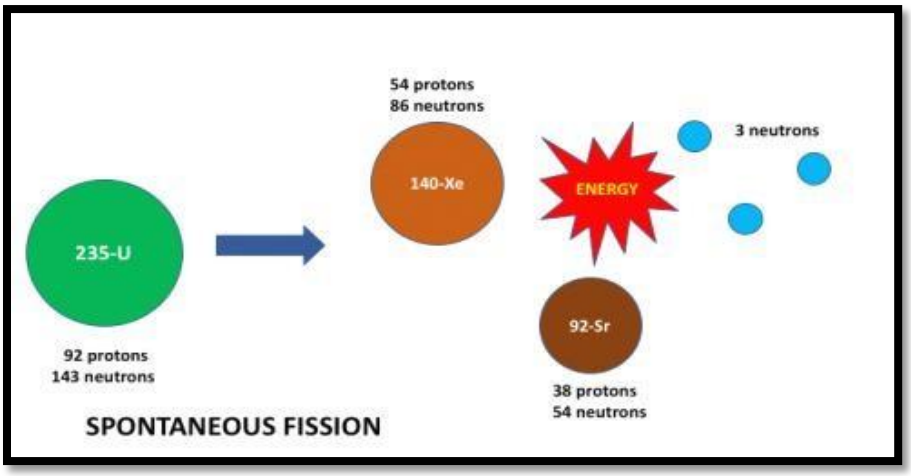


**Figure 1.4** Spontaneous fission of $^{235}U$.

Figure 4 depicts an isotope of Uranium i.e. $^{235}U$ after decaying via spontaneous fission (radioactive decay) and it ejects two daughter nuclei, 3 neutrons, and energy.

The most prominent decay modes in case of superheavy elements are spontaneous fission and alpha decay. The half lives of alpha decay are more as compared to half lives in case of spontaneous fission. The spontaneous fission process is very much complex as it has so many uncertainties like charge and mass of the ejecting fragments, number of neutrons etc.

All the nuclei are bonded together with a force known as nuclear force. The magnitude of force with which these nucleons interact with each other can be determined by calculating the binding energies of nuclei. For instance, the binding energy of nuclei that lie on the valley of stability is very high and radioactive nuclei have significantly low binding energies. The half life times of radioactive nuclei can be computed using binding energy with which the nucleons inside the nuclei are packed. These nuclear models can be used to determine the binding energies of nucleus.

## 1.4 Nuclear models

Several models were developed which helped Niels Bohr to come up with the quantum theory which could describe how nucleus work. So many predictions were made to provide the information about the properties of atomic nuclei on the basis of these models. The liquid drop model which assumed nucleus as a drop of liquid containing nucleons held tightly by a force between them known as nuclear force (the strongest known force). But unfortunately, the liquid drop model was incapable to incorporate about the deformation of nucleus, shell effects, magic number and hence the stability of nucleus. So a new model came into picture which was able to unfold the properties and effects that the liquid drop model could not. The shell model assumed the pairing of nucleons present in different energy states within the nucleus. It was able to predict the shell effects, the magic numbers (2, 8, 20, 28, 50, 82 and 126), the angular momentum, spin of particles and the change in binding energy given by liquid drop model due to shell corrections successfully.

Three fundamental models have been developed to anticipate the properties of nuclei: liquid drop model, shell model and collective model. Here we will confine ourselves to liquid drop model and shell model.

### 1.4.1 Liquid Drop Model

George Gamow contributed the liquid drop model in the development of nuclear physics. Atomic nucleus has an analogy with drop of liquid and all nucleons are bounded with strong nuclear force. This was the very first successful model to anticipate the binding energies and masses of nuclei. The energy employed to pull the nucleus apart and to divide it into fragments is binding energy of the nucleus. Binding energy has dependence on mass number (A) and atomic number (Z). The macroscopic part of binding energy is determined using semi empirical mass formula or Bethe-Weizsacker formula *i.e.*

- **Volume term:** the interaction among the nucleons packed up deep inside the nucleus (within the volume) contributes to binding energy.
- **Surface term:** When nucleons present on the surface of nucleus interacts with each other. This term is small in comparison to volume term as numbers of nucleons on the surface are less.
- **Coulomb term:** This term comes into picture due to electrostatic repulsion between the protons.
- **Asymmetry term:** The asymmetry that arises due to more number of neutrons and not well defined energy states for them.
- **Pairing term:** This term arises due to the pairing forces between the two neutrons or two protons.

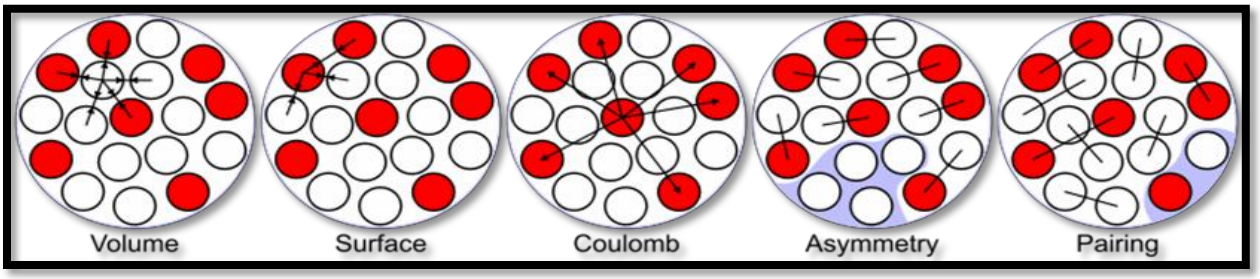


**Figure 1.5** Different interactions between the nucleons.

Figure 1.5 depicts the different ways in which nucleons can interact with each other and amalga --mations of all these interactions give rise to binding energy according to liquid drop model.

### 1.4.1(a) Why liquid drop Model failed?

- This model was solely based on classical approach and could contribute only macroscopic term. It could not incorporate about the shell structure of the nuclei and hence the inclusion of microscopic term became mandatory to anticipate the effects of shell corrections.
- It failed to elucidate the stability of many nuclei having magic number of protons or neutrons.
- The binding energies predicted for lighter nuclei were not in agreement with experimental ones.
- Pairing effect could not be unlocked using liquid drop model.

These inadequacies of the liquid drop model are taken care by the shell model that is discussed below.

### 1.4.2 Shell Model

As the liquid drop model was unable to explain every property of the nucleus, a more advanced model was needed. Shell model was developed in 1932 by Dmitri Ivanenko (together with E.Gapon). According to shell model, the energies are distributed in shells and the nucleons are distributed in these discrete energy levels. Shell model employed Pauli Exclusion Principle. This model was found successful in explaining the shell structures by including some shell corrections. The magic numbers were inculcated i.e. if the number of protons or neutrons are 2,8,20,28,50,82 then that nucleus would be called as magic nucleus and is comparatively more stable. Hence this model very well incorporates the stability of nuclei.

- The birth of magic numbers was found as a remarkable tool in calculating shell corrections.
- Binding energies determined after inculcation of microscopic term were in agreement with the experimental values.

## 1.5 Shell Corrections

If one talk about heavier species, more number of shells are added because of plenty number of nucleons. Shell structures start deviating from their original shell structure drastically. Hence the role of shell effect cannot be ignored. Shell correction becomes utmost important as we approach heavier masses because it helps in investigation of shell structures. The irregular distribution of

nucleons is responsible for the shell corrections. Binding energies that were examined earlier did not take shell effects into account. In heavier mass region amalgamation of microscopic terms with macroscopic terms (one obtained from liquid drop model) becomes mandatory [5]. Masses examined by the liquid drop model deviate extensively from their experimental values as shell effects and etc were not taken into account. To correct this deviation, microscopic terms that include the role of shell effects were added.

We used Myers and Swiatecki approach [6] to inculcate microscopic terms (shell correction). Shell corrections were added to observe the mass deviation bumps in magic numbers and flat bumps along with deformations. By incorporating effects of shell, the overall binding energy changes and drastic changes can be seen in radioactive nuclei. This method is evident for $Z \geq 16$.

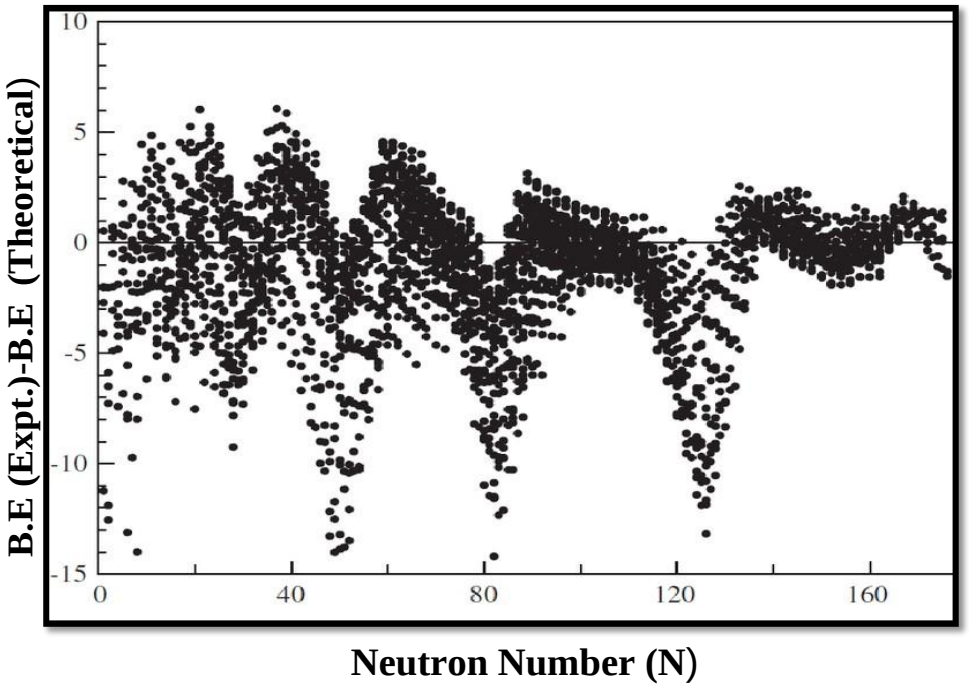


**Figure 1.6** The shell corrections are depicted i.e. variation between experimental and theoretical (obtained from liquid drop model) binding energy as a function of N (number of neutrons).

Figure 1.6 depicts the shell correction energy *i.e.* the difference in experimental and theoretical binding energy as function of neutron number N. The shell correction energy shows positive as well the negative effects ranging from -15 MeV to 5 MeV (approximately). The negative values of shell corrections correspond to the shell closure and as we move away from the shell closure, the shell correction energy comes out to be positive.

## 1.6 Literature Review

Shell correction has great importance in mesoscopic studies i.e. the studies intermediate between microscopic and macroscopic systems. Shell correction is a mandatory tool in evaluating nuclear fission barriers as well. The shell corrections holds abundant applications, hence good amount of work has been done to study more effects related to shell corrections which are as follows:

- The changes in potential energy surfaces have been examined with inclusion and non-inclusion of shell correction term when investigating the role of orientations in cluster decay having doubly magic daughter fragments ($^{120}$Sn and $^{132}$Sn) which in turn helped us in examining how doubly magic shell configuration of fragments is of keen importance [11].
- The importance of shell corrections is reviewed for examining the energetics of heavy particle radioactivity in clusterization of superheavy nuclei in ground state having Z=113, 115 and 117 [12].
- Further, shell correction enhances the calculated α-decay half lives for the nuclei $^{292\text{-}298}$Fl because the shell effects are pronounced for these nuclei [7].
- The survival of shell stabilized nuclei and the exact position of the magic numbers on the nuclear chart is being investigated from last forty years [10]. One such estimate is the spherical doubly-magic superheavy nucleus island of stability using the macro-micro approach [9].
- It has been reported that negative shell correction leads to fusion hindrance, whereas positive shell correction results in the weak enhancement of the fusion cross-sections in the deep sub-barrier region [10]. In this study, the shell corrections are added to the nucleon-nucleon potential.

The Preformed Cluster Model (PCM) [11-17] which has been developed by Gupta and collaborators for studying the dynamics of radioactive nuclei in heavier mass region employs a simple idea that the daughter fragments ejected out are preborn in the parent nuclei and comes out by tunneling off the barrier. In the next chapter, we will discuss the methodology i.e. how PCM actually works in detailed manner and what role shell correction term plays when calculating the binding energies.

# *Chapter 2*

# *Methodology*

## 2.1 Preformed Cluster-decay Model (PCM)

In the present work, Preformed Cluster decay-Model (PCM) [11-17] is used to study the spontaneous fission. In PCM, it is considered that clusters or fragments are preborn in their parent nucleus with different probabilities of preformation and their ejection takes place via tunneling across the barrier. This model gives us the basic information about the fragments that are being ejected out. It also includes the associated structure effect of the nuclei as well. It is based on the quantum mechanical fragmentation theory (QMFT). The concept of quantum tunneling, which is responsible for penetrating the barrier (penetration probability), is used for determining half lives of the clusters.

Various phenomenon of the nuclei in their ground state can be studied using this model like alpha decay, cluster decay, heavy ion fission reaction etc. The PCM has been found to be successful in calculating half lives of various nuclei taking preformation probability and penetrability into account. In addition to that the structural information of nuclei like role of shell correction in heavier mass region, modification of barrier has also been studied.

The half lives calculated using PCM [11-17] depends on:

* The cluster preformation probability $P_0$.
* The barrier impinging frequency $\nu_o$.
* The barrier penetrability P.

The half life of radioactive species is denoted by $T_{1/2}$ i.e. the time employed to disintegrate half of the nucleus. The decay constant $\lambda$ is related to $T_{1/2}$ as [11-17]:

$$\frac{\quad}{\quad} \qquad (1)$$

$$\lambda = \nu_o P P_0 \qquad (2)$$

The barrier impinging frequency $\nu_o$ is given simply as,

$$\nu_o = \frac{}{}$$

$$= \frac{}{}, \quad \mu \text{ is reduced mass of two fragment} \tag{3}$$

$$E_2 = \frac{}{}, \quad A \text{ is mass of parent nucleus.} \tag{4}$$

Here $E_2$ is kinetic energy of one of the daughter fragment that has been penetrated out and $R_0$ is radius of parent nuclei. The value of impinging frequency is $10^{21}$ $s^{-1}$ which is taken from experimental Q value and is approximately same for all spontaneous decays. This Q value is total kinetic energy that is distributed among fragments that are ejected out. Hence, Q = $E_1$+$E_2$, $E_1$ be the energy of daughter fragment [11].

## 2.2 Preformation Probability ($P_0$)

The probability of formation of fragments inside the parent nucleus is called preformation probability. The preformation probability is different for different fragments and it depends on the mass of nuclei. The structural information of the parent nucleus is provided by preformation probability and is calculated by solving Schrödinger equation in mass asymmetry ($\eta$) and fragmentation potential $V_R$, defined later.

Schrödinger wave equation in terms of mass parameters η and relative separation R co-ordinates for the potential V (η ,R) is given below:

$$H(\eta, R)\,\psi(\eta, R) = E\,\psi(\eta, R) \tag{5}$$

Eq. (5) is solved in the decoupled approximation $\psi^{\nu}(\eta,R) = \psi^{\nu}(\eta)\,\psi^{\nu}(R)$. Here, $\eta = (A_1-A_2)/(A_1+A_2)$ [21], and is defined in dynamical collective coordinates having coupled motion.

The solution of Eq. (5) at $R=R_a$ comes out to be [15, 20]:

$$\frac{}{} \quad \frac{}{} \quad (\eta) \tag{6}$$

$R_a$ is the first turning point i.e. the point where tunneling begins. The vibrational states corresponding to $V_R$ (η) are represented by . ν =0, 1, 2, 3…..refers to ground state solution (ν =0) and solution of excited states.

Here $R = R_a = R_t + \Delta R$, $R_t = R_1 + R_2$, where ΔR is neck length parameter *i.e.* when two fragments are on the verge of separation, a neck is formed between the two fragments.

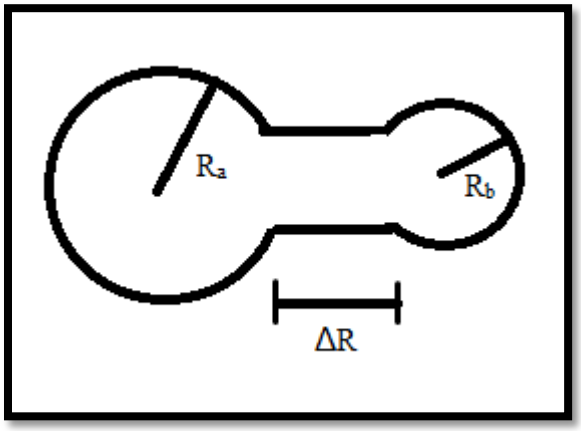


**Figure 2.1** Formation of neck when parent nucleus disintegrates into its daughter fragments.

Figure 2.1 depicts the formation of neck having length ΔR (neck length parameter) when parent nucleus splits into its daughter fragments with radius $R_a$ and $R_b$.
The length of the neck formed is neck length. $R_1$ and $R_2$ are radii of two fragments. In this method, R is the sole variable and is known to be effective sharp radius [16].

$$(i=1, 2\ldots.) \qquad (7)$$

If we incorporate the surface effects as well then we denote it by C

$$C = C_1 + C_2 + \Delta R, \quad C_t = C_1 + C_2$$

$\_$ , $C_i$ is Süssmann central radius [15].

For the spontaneous fission, only ground state solutions i.e. T = 0, ν = 0 are relevant.

Hence, the ground state $P_0$ is given as

$$P_0 = \left| \quad \right| \quad \frac{}{} \_ , \qquad B_{\eta\eta} \text{ is mass parameter.} \qquad (8)$$

## 2.3 Penetration Probability (P)

The parent nucleus has some definite value of potential barrier which resists its fragments to come out of the nucleus or undergo fission. Hence the ability of nuclei to penetrate that barrier and undergo fission is given by the term penetration probability P. The daughter nuclei inside the parent nucleus hits the surface of parent atom with certain frequency and finally tunnels through the potential barrier. The penetration probability in PCM is a three step process and is calculated by WKB approximation [11, 13]. Beginning from the first turning point $R_a$ to the position where the potential is equal to the Q-value, the penetration probability comprises of following three steps [20]:

, (8a)

— , (8b)

— (8c)

$W_i$ is the probability of de-excitation between $P_i$ and $P_b$ and is equal to unity. It shows that tunneling initiates with $R=R_a$ (first turning point) and finishes at $R=R_b$ (second turning point) where $V(R_b)$ =Q value.

## 2.4 Fragmentation Potential $V_R(\eta)$

in Eq.(5) is given as :

$$V_R(\eta) = \frac{}{} \_\_\_\_ \qquad (9)$$

The first term in the above equation signifies the binding energy of the two fragments. The second term represents the Coulomb interaction. $V_l$ and $V_p$ are the centrifugal and proximity nuclear potentials respectively.

## 2.5 Binding Energy

Myers-Swiatecki [6] proposed a two part approach i.e. the binding energy is written in the form in which first term corresponds to the macroscopic term and other term is microscopic term.

(10)

The first part is the macroscopic term which is defined using semi-empirical mass formula or Bethe-Weizsacker formula based on liquid drop model and it does not have the shell effects. The macroscopic term in Eq. (10) is defined as:

(11)

Here, $a_v$ is the volume coefficient, is the surface coefficient, is the coulomb term coefficient and is asymmetry term coefficient.

The binding energies predicted using above formula did not coincide the experimental values. Hence, a correction term was mandatory to include shell effects as well.

## 2.6 Shell Correction Energy

The semi empirical mass formula was capable in providing us the good idea about atomic masses and various other effects but it could not incorporate with the extra binding energy term which help in defining the stability of nuclei considering the shell effects, deformation effects, *etc*. The microscopic parts in Myers-Swiatecki approach [6] lead us to shell corrections. The shell correction $\delta U$ term (microscopic term) is added to observe the following:

- Bumps in Mass deviation between the magic numbers.
- Flattened bumps along with deformations.

The microscopic term in Eq.(10) is given by [21]:

(12)

In Eq. (12) X=Z or N, $M_{i-1}<X<M_{i,.}$ $M_i$ is the magic number (2, 8, 20, 28, 50, 82, and 126), (D=5.8 MeV and c = 0.26).

Nucleus is spherical near shell closure or at magic number; hence the value of δU is negative. As we move away from shell closure or magic numbers the value of δU is positive

If $\delta U>0$, then $BE_{\text{shell correction}} > BE_{\text{LDM}}$.

If $\delta U<0$, then $BE_{\text{shell correction}} < BE_{\text{LDM}}$.

Hence due to inclusion of the shell corrections, the binding energy gets modified which changes the fragmentation potential due to which preformation probability alters and hence the half life of the nuclei.

In the next chapter, we will study how these shell corrections affect the probability of preformation of daughter fragments and fragmentation potential of various parent nuclei particularly $^{232}U$ to $^{264}Hs$ undergoing spontaneous fission within the collective clusterization approach of the PCM [11-17] and how the half lives of parent nuclei gets affected if we exclude the shell corrections.

# *Chapter 3*

## *Results and Discussion*

The role of shell corrections (δU) on half life times of various parent nuclei undergoing spontaneous decay has been explored in this chapter. The Preformed Cluster-decay Model has been employed in the present study. The calculations are done in view of available experimental data [13]. We have extended the previous study in which the spontaneous fission half lives are fitted using the neck length parameter ΔR in the presence of shell correction energy (δU≠0). Using the same neck-length, the influence of shell corrections on spontaneous fission half lives and other parameters has been analyzed.

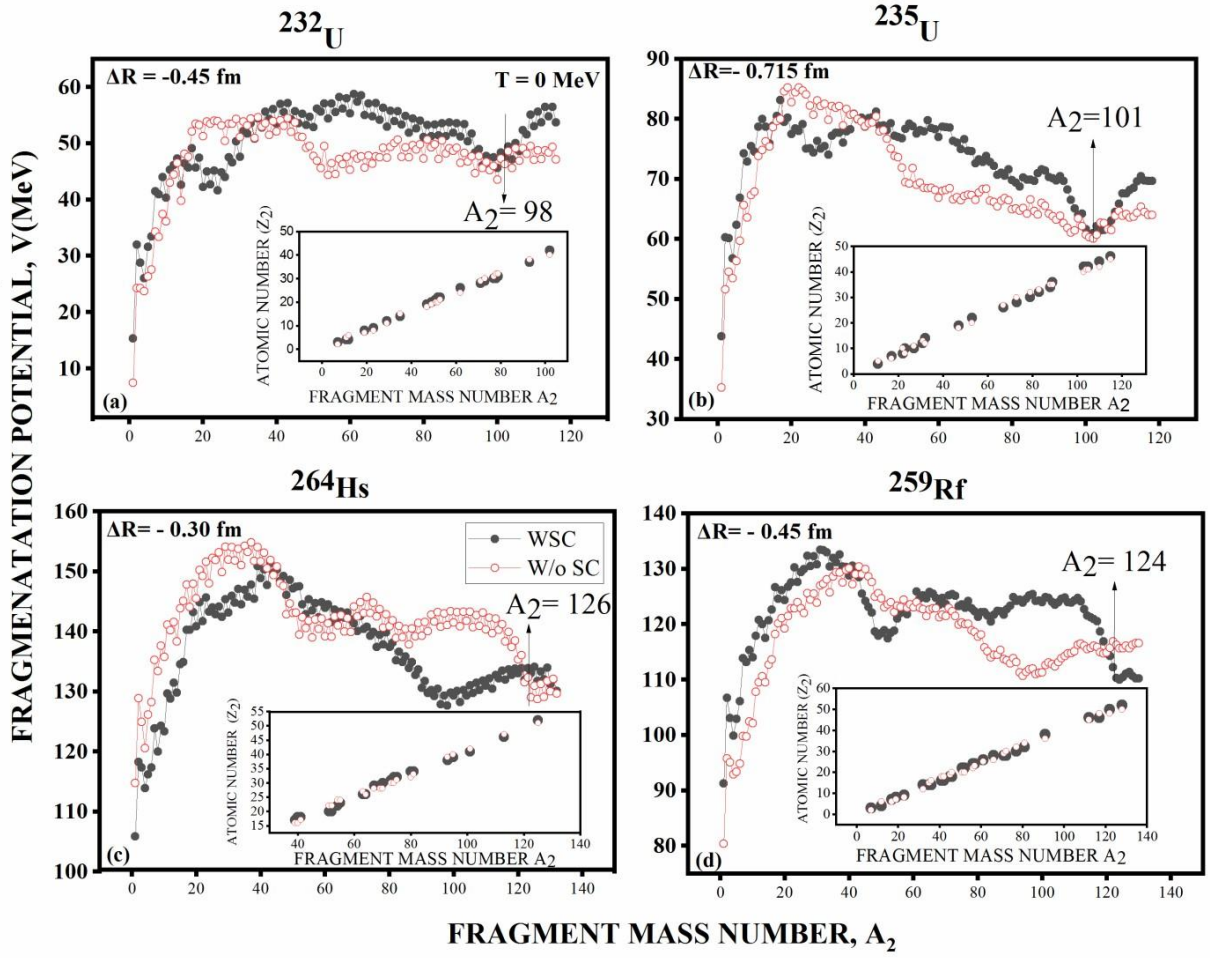


**Figure 3.1** The deviation in fragmentation potentials with (WSC) and without shell correction energy (W/o SC) is plotted against fragment mass number ($A_2$) for four cases: (a) $^{232}$U (b) $^{235}$U (c) $^{264}$Hs

(d) $^{259}$Rf. The corresponding variation of atomic number under the effect of shell corrections is depicted in the inset. The fitted $\Delta R_s$ are taken from Ref. [13].

Figure 3.1 depicts the variation in fragmentation potentials Ref. [15] plotted against fragment mass number ($A_2$) using $\delta U=0$ and $\delta U\neq 0$. We have considered four cases: (a) $^{232}$U, (b) $^{235}$U, (c) $^{264}$Hs, (d) $^{259}$Rf. Fragmentation potential shows positive as well as negative effects when shell corrections are switched off but in most of the mass region fragmentation potential decreases when shell corrections are not included. Fragmentation potential has increment in some region in absence of shell correction. It increases for $A_2$=15-36 when $^{232}$U is taken into consideration. $A_2$=18-36, 104-105 in case of $^{235}$U. For$^{264}$Hs, this mass region is widespread i.e. $A_2$=1-45, 69-121, 131-132. Similarly for $^{259}$Rf, $A_2$=40-59, 120-130 have higher fragmentation potential when shell corrections are switched off.

The inset in the figure 3.1 shows the change in atomic mass number of fragments while including and excluding the shell correction energy which is shown in table 31. It has been observed that after switching off shell correction energy the atomic number of few fragment changes. Hence shell correction is affecting the fragmentation potential as well as atomic number of some of the fragments.

Figure 3.2 depicts the variation of preformation probability with (WSC) and without including shell correction energy (W/o SC) for four cases: (a) $^{232}$U, (b) $^{235}$U, (c) $^{264}$Hs and (d) $^{259}$Rf. The corresponding neck length $\Delta R_s$ are also depicted in the figure 3.2. Clear differences are observed in the preformation probability because of the corresponding variations in the fragmentation potential which depends on binding energy and hence shell correction energy. Also, the preformation probability is a relative factor, and its magnitude is dependent upon the relative contribution of all the decaying fragments and not only on the individual decay channel due to the collective clusterization procedure followed in the PCM. The preformation probability decreases when shell corrections are switched off for maximum number of fragments. The effects of shell correction energy of all the fragments are clearly reflected in the preformation factor here. Although the shell corrections found to have maximum positive effects on the preformation probability, it is of further interest to see its effect on the spontaneous fission half lives.

**Table 1** Change in the atomic no. of outgoing fragments while excluding the shell corrections as shown in the inset of figure 3.1 are tabulated here.

| $^{232}$U | | $^{235}$U | | $^{264}$Hs | | $^{259}$Rf | |
|---|---|---|---|---|---|---|---|
| **WSC** | **W/o SC** | **WSC** | **W/o SC** | **WSC** | **W/o SC** | **WSC** | **W/o SC** |
| $^{7}$Li+$^{225}$Ac | $^{7}$He+$^{225}$Th | $^{11}$Be+$^{224}$Ra | $^{11}$B+$^{224}$Fr | $^{39}$Cl+$^{225}$Pa | $^{39}$S+$^{225}$U | $^{7}$Li+$^{252}$Md | $^{7}$He+$^{252}$No |
| $^{11}$Be+$^{221}$Ra | $^{11}$B+$^{221}$Fr | $^{17}$N+$^{218}$At | $^{17}$C+$^{218}$Rn | $^{40}$Ar+$^{224}$Th | $^{40}$S+$^{224}$U | $^{12}$Be+$^{247}$Fm | $^{12}$C+$^{247}$Cf |
| $^{12}$Be+$^{220}$Ra | $^{12}$C+$^{220}$Rn | $^{22}$O+$^{213}$Po | $^{22}$Ne+$^{213}$Pb | $^{41}$Ar+$^{223}$Th | $^{41}$Nb+$^{223}$Pa | $^{17}$N+$^{242}$Bk | $^{17}$C+$^{242}$Cf |
| $^{19}$O+$^{213}$Po | $^{19}$N+$^{213}$At | $^{23}$Ne+$^{212}$Pb | $^{23}$O+$^{212}$Po | $^{51}$Ca+$^{213}$Ra | $^{51}$Ti+$^{213}$Rn | $^{19}$O+$^{240}$Cm | $^{19}$N+$^{240}$Bk |
| $^{23}$F+$^{209}$Bi | $^{23}$O+$^{209}$Po | $^{27}$Ne+$^{208}$Pb | $^{27}$Na+$^{208}$Tl | $^{52}$Ca+$^{212}$Ra | $^{52}$Ti+$^{212}$Rn | $^{23}$F+$^{236}$Am | $^{23}$O+$^{236}$Cm |
| $^{29}$Mg+$^{203}$Hg | $^{29}$N+$^{203}$Tl | $^{31}$Mg+$^{204}$Hg | $^{31}$Al+$^{204}$Au | $^{54}$Ti+$^{210}$Rn | $^{54}$Cr+$^{210}$Po | $^{32}$Si+$^{227}$Th | $^{32}$Mg+$^{227}$U |
| $^{35}$Si+$^{197}$Pt | $^{35}$P+$^{197}$Ir | $^{32}$Si+$^{203}$Pt | $^{32}$Mg+$^{203}$Hg | $^{55}$V+$^{210}$At | $^{55}$Cr+$^{210}$Po | $^{35}$Si+$^{224}$Th | $^{35}$P+$^{224}$Ac |
| $^{47}$K+$^{185}$Ta | $^{47}$Ar+$^{185}$W | $^{47}$K+$^{188}$Ta | $^{47}$Ar+$^{188}$W | $^{63}$Fe+$^{201}$Pb | $^{63}$Co+$^{201}$Tl | $^{36}$Si+$^{223}$Th | $^{36}$S+$^{223}$Ra |
| $^{49}$Ca+$^{183}$Hf | $^{49}$K+$^{183}$Ta | $^{53}$Ti+$^{182}$Yb | $^{53}$Ca+$^{182}$Hf | $^{64}$Fe+$^{200}$Pb | $^{64}$Fe+$^{200}$Pb | $^{41}$S+$^{218}$Ra | $^{41}$Ar+$^{218}$Rn |
| $^{51}$Sc+$^{181}$Lu | $^{51}$Ca+$^{181}$Hf | $^{67}$Fe+$^{168}$Dy | $^{67}$Co+$^{168}$Tb | $^{67}$Cu+$^{197}$Au | $^{67}$Ni+$^{197}$Hg | $^{42}$S+$^{217}$Ra | $^{42}$Ar+$^{217}$Rn |
| $^{52}$Ti+$^{180}$Yb | $^{52}$Ca+$^{180}$Hf | $^{73}$Ni+$^{162}$Gd | $^{73}$Zn+$^{162}$Sm | $^{69}$Cu+$^{195}$Au | $^{69}$Ni+$^{195}$Hg | $^{45}$Ar+$^{214}$Rn | $^{45}$K+$^{214}$At |
| $^{53}$Ti+$^{179}$Yb | $^{53}$Sc+$^{179}$Lu | $^{79}$Zn+$^{156}$Sm | $^{79}$Ge+$^{156}$Nd | $^{70}$Zn+$^{194}$Pt | $^{70}$Ni+$^{194}$Hg | $^{46}$Ar+$^{213}$Rn | $^{46}$Ca+$^{213}$Po |
| $^{62}$Fe+$^{170}$Dy | $^{62}$Cr+$^{170}$Er | $^{83}$Ge+$^{152}$Nd | $^{83}$As+$^{152}$Pr | $^{73}$Ga+$^{191}$Ir | $^{73}$Zn+$^{191}$Pt | $^{51}$Ti+$^{208}$Pb | $^{51}$Ca+$^{208}$Po |
| $^{71}$Ni+$^{161}$Gd | $^{71}$Cu+$^{161}$Eu | $^{88}$Se+$^{147}$Ce | $^{88}$Br+$^{147}$La | $^{74}$Ge+$^{190}$Os | $^{74}$Zn+$^{190}$Pt | $^{52}$Ti+$^{207}$Pb | $^{52}$Ca+$^{207}$Po |
| $^{73}$Cu+$^{159}$Eu | $^{73}$Zn+$^{159}$Sm | $^{89}$Kr+$^{146}$Ba | $^{89}$Br+$^{146}$La | $^{75}$Ge+$^{189}$Os | $^{75}$Ga+$^{189}$Ir | $^{56}$Cr+$^{203}$Hg | $^{56}$Ti+$^{203}$Pb |
| $^{77}$Zn+$^{155}$Sm | $^{77}$Ga+$^{155}$Pm | $^{103}$Mo+$^{132}$Sn | $^{103}$Zr+$^{132}$Te | $^{80}$Se+$^{184}$W | $^{80}$Ge+$^{184}$Os | $^{57}$Cr+$^{202}$Hg | $^{57}$V+$^{202}$Tl |
| $^{78}$Z+$^{154}$Sm | $^{78}$Ge+$^{154}$Nd | $^{104}$Mo+$^{131}$Sn | $^{104}$Nb+$^{131}$Sb | $^{81}$Se+$^{183}$W | $^{81}$As+$^{183}$Re | $^{61}$Fe+$^{198}$Pt | $^{61}$Mn+$^{198}$Au |
| $^{79}$Ga+$^{153}$Pm | $^{79}$Ge+$^{153}$Nd | $^{105}$Mo+$^{130}$Sn | $^{105}$Nb+$^{130}$Sb | $^{93}$Sr+$^{171}$Yb | $^{93}$Y+$^{171}$Lu | $^{66}$Ni+$^{193}$Os | $^{66}$Fe+$^{193}$Pt |
| $^{93}$Rb+$^{139}$Cs | $^{93}$Sr+$^{139}$Xe | $^{110}$Ru+$^{125}$Cd | $^{110}$Mo+$^{125}$Sn | $^{95}$Y+$^{169}$Lu | $^{95}$Zr+$^{169}$Er | $^{71}$Ni+$^{188}$Os | $^{71}$Cu+$^{188}$Re |
| $^{102}$Mo+$^{130}$Sn | $^{102}$Zr+$^{130}$Te | $^{115}$Pd+$^{120}$Pd | $^{115}$Rh+$^{120}$Ag | $^{101}$Nb+$^{163}$Ho | $^{101}$Mo+$^{163}$Dy | $^{72}$Ni+$^{187}$Os | $^{72}$Zn+$^{187}$W |
| | | | | $^{113}$Pd+$^{151}$Sm | $^{113}$Ag+$^{151}$Pm | $^{77}$Zn+$^{182}$W | $^{77}$Ge+$^{182}$Hf |
| | | | | $^{125}$Te+$^{139}$Ba | $^{125}$Sb+$^{139}$La | $^{81}$Ge+$^{178}$Hf | $^{81}$Se+$^{178}$Yb |
| | | | | | | $^{91}$Sr+$^{168}$Dy | $^{91}$Kr+$^{168}$Er |
| | | | | | | $^{112}$Pd+$^{147}$Ce | $^{112}$Rh+$^{147}$Pr |
| | | | | | | $^{117}$Pd+$^{142}$Ce | $^{117}$Cd+$^{142}$Ba |
| | | | | | | $^{122}$Sh+$^{137}$Xe | $^{122}$Cd+$^{137}$Ba |
| | | | | | | $^{128}$Te+$^{131}$Te | $^{128}$Sn+$^{131}$Xe |

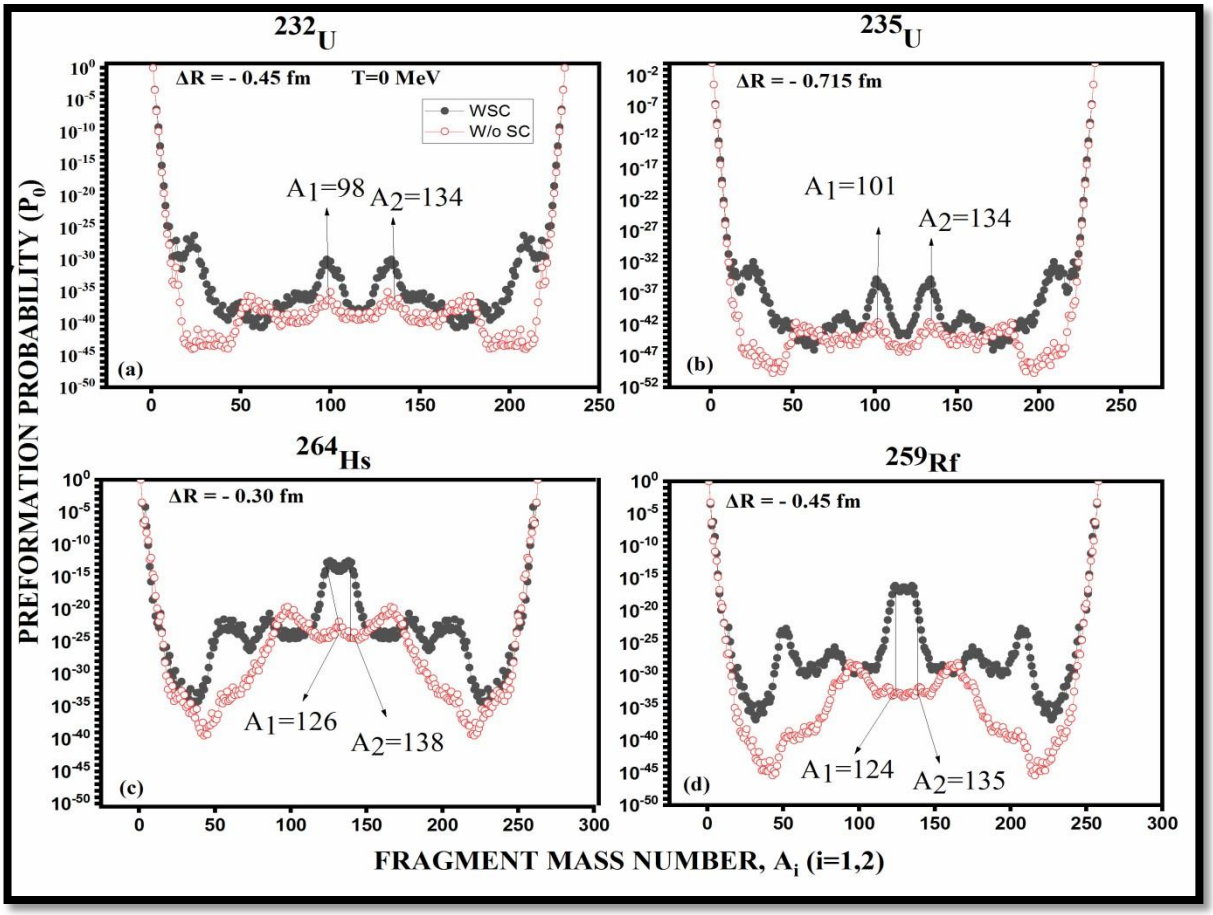


**Figure 3.2** The variation in preformation probability ($P_0$) with (WSC) and without shell correction energy (W/o SC) is plotted against fragment mass number $A_i$ for the same cases as in figure 3.1.

Figure 3.3 depicts the preformation probability ($P_0$) of decaying channel of various parent nuclei with (WSC) and without shell correction energy (W/o SC). We have considered four cases: (a) Even Nuclei ($R_t$) ($^{232}$U, $^{234}$U, $^{236}$U, $^{238}$U, $^{240}$Pu, $^{250}$Fm, $^{252}$Fm), (b) Odd Nuclei ($R_t$) ($^{255}$Lr, $^{253}$Es, $^{249}$Cf, $^{249}$Bk, $^{245}$Cm, $^{243}$Cm, $^{243}$Am, $^{241}$Pu), (c) Even Nuclei ($C_t$) ($^{254}$Fm, $^{256}$Fm, $^{256}$No, $^{258}$Rf, $^{258}$Sg, $^{260}$Sg, $^{262}$Sg, $^{264}$Hs), (d) Odd Nuclei ($C_t$) ($^{255}$Md, $^{257}$Lr, $^{257}$Md, $^{257}$No, $^{259}$Lr, $^{259}$Md, $^{259}$No, $^{259}$Rf). $R_t$ and $C_t$ describe the choice of radius for the nuclei. The corresponding decaying channels are marked in the figure. The relative change in the preformation probabilities of individual decaying channels with and without shell correction energy is evident. Deviation in preformation probability with and without shell correction energies varies from order of 6 to order of 20. When we switch off the shell corrections, the change in atomic number of daughter fragment has also been observed which are marked in the plot. There is no change in atomic number of

daughter fragment for the parents plotted in case (c). Further, the disappearance of magicity has also been observed in some cases when we exclude the shell correction energy. In case (a) of figure 3.3 $^{248}$Cm decayed into $^{116}$Pd + $^{132}$Sn with shell corrections, after excluding shell correction energy decaying channel alters to $^{116}$Ru + $^{132}$Te. $^{132}$Sn has 82 neutrons and 50 protons (magic nucleus) but $^{132}$Te has 80 neutrons and 52 protons (not magic nucleus). Hence it is observed that when the shell corrections are switched off then magicity of fragment vanishes. In some cases only neutron magicity vanishes. As an example, in case (a) of figure 3.3 $^{136}$Xe, the daughter fragment of $^{256}$Lr (parent nuclei) has 82 neutrons, after excluding shell corrections, the daughter fragment changes into $^{136}$Cs and has 81 neutrons. In case (b) $^{245}$Cm witnesses change in proton magicity.

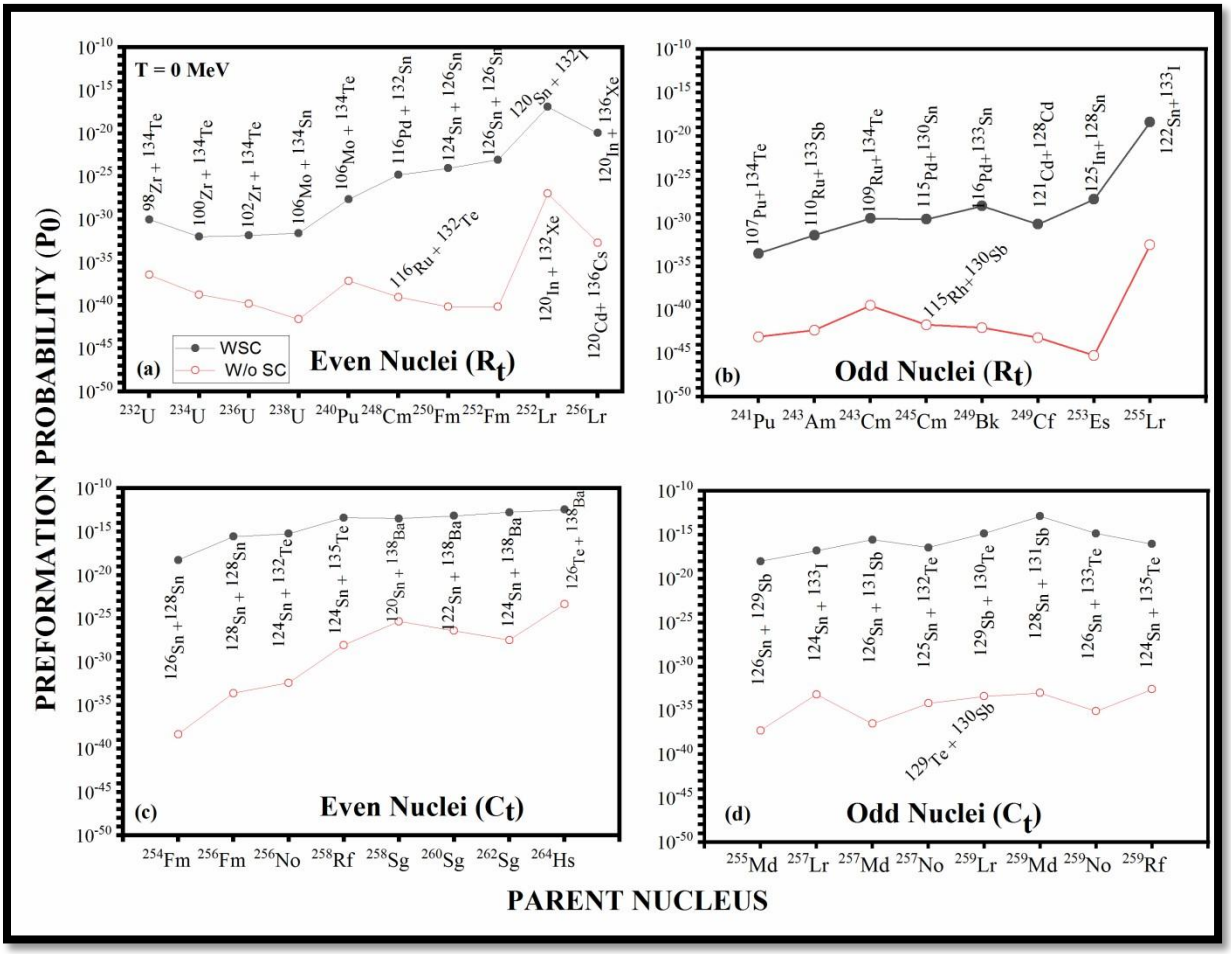


**Figure 3.3** The preformation probability ($P_0$) is plotted for decaying channel of different parent nuclei in case of (a) Even Nuclei ($R_t$), (b) Odd Nuclei ($R_t$), (c) Even Nuclei ($C_t$), (d) Odd Nuclei $C_t$) with (WSC) and without shell corrections (W/o SC). The change in atomic number of daughter nuclei after switching off shell corrections is also marked in the graph. Here $R_t$ and $C_t$ describe the choice of radius of the nuclei.

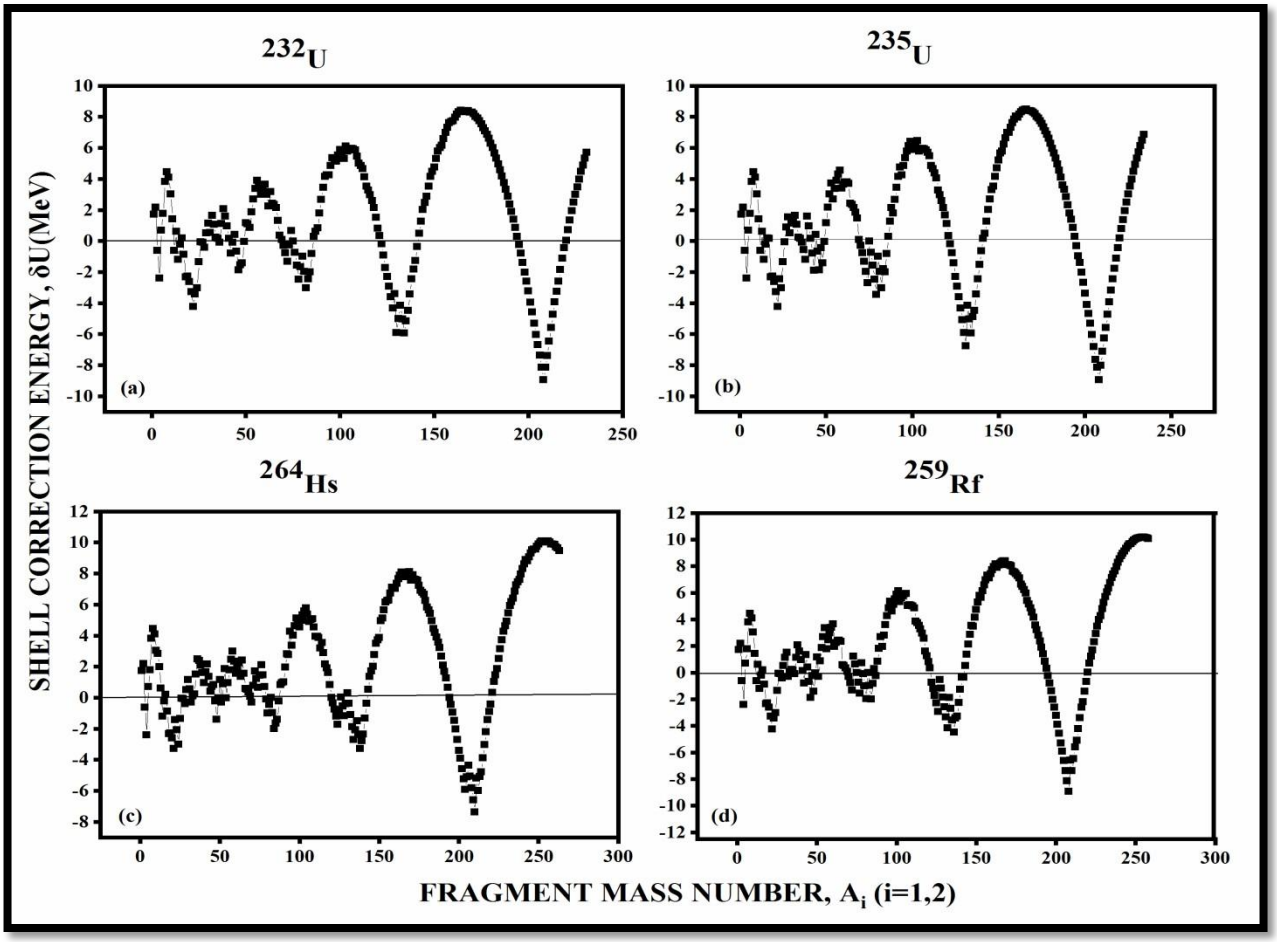


**Figure 3.4** The plots of shell correction energy (δU) against the fragment mass number for various parent nuclei: (a) $^{232}$U, (b) $^{235}$U, (c) $^{264}$Hs, (d) $^{259}$Rf.

Figure 3.4 depicts the variation in shell correction energy (δU) with the mass number of fragments for four cases: (a) $^{232}$U, (b) $^{235}$U, (c) $^{264}$Hs, (d) $^{259}$Rf. The shell correction energy is the difference of experimental binding energy and binding energy calculated from the liquid drop model. Shell correction energy can be positive as well as negative is clear from the figure 3.4. The minima and maxima of shell correction energy correspond to -7.375 MeV and 10 MeV respectively. The magnitude of the shell correction energy is high, that is why preformation probability changes drastically. With the increase in the mass of the fragment/nuclei, the shell correction energy is required to be added to the macroscopic term of the binding energy in order to attain the stability. The peaks and dips in the plots depict the vicinity of magic numbers. Near the shell closure or at magic numbers the value of shell correction energy is negative, as we move away from surface or shell, the magic numbers start vanishing and δU becomes positive.

**Table 2** The calculated half life times of various parent nuclei with WSC and without shell corrections energy has been compared. Corresponding experimental half life times are also listed.

| Serial No. | Parent Nucleus | Decay channel | Choice of Radius | ΔR (fm) | $\log T_{1/2}$(sec) (PCM) | | Expt. |
|---|---|---|---|---|---|---|---|
| | | | | | W/o SC | WSC | |
| 1. | $^{232}$U | $^{98}$Zr + $^{134}$Te | $R_t$ | -0.45 | 30.55 | 21.54 | 21.39 |
| 2. | $^{234}$U | $^{100}$Zr + $^{134}$Te | $R_t$ | -0.594 | 33.26 | 23.62 | 23.67 |
| 3. | $^{235}$U | $^{101}$Zr + $^{134}$Te | $R_t$ | -0.715 | 37.00 | 26.63 | 26.49 |
| 4. | $^{236}$U | $^{102}$Zr + $^{134}$Te | $R_t$ | -0.67 | 35.16 | 23.85 | 23.89 |
| 5. | $^{238}$U | $^{102}$Mo + $^{134}$Sn | $R_t$ | -0.63 | 37.84 | 23.31 | 23.41 |
| 6. | $^{239}$Pu | $^{105}$Mo + $^{134}$Te | $R_t$ | -0.595 | 35.72 | 23.21 | 23.39 |
| 7. | $^{240}$Pu | $^{106}$Mo + $^{134}$Te | $R_t$ | -0.38 | 31.30 | 18.13 | 18.17 |
| 8. | $^{241}$Pu | $^{107}$Mo + $^{134}$Te | $R_t$ | -0.69 | 38.47 | 24.65 | 24.36 |
| 9. | $^{243}$Am | $^{110}$Ru + $^{133}$Sb | $R_t$ | -0.65 | 37.80 | 21.80 | 21.79 |
| 10. | $^{243}$Cm | $^{109}$Ru + $^{134}$Te | $R_t$ | -0.45 | 33.45 | 19.32 | 19.23 |
| 11. | $^{245}$Cm | $^{115}$Pd + $^{130}$Sn | $R_t$ | -0.50 | - | 19.40 | 19.64 |
| 12. | $^{248}$Cm | $^{116}$Pd + $^{132}$Sn | $R_t$ | -0.40 | - | 14.02 | 14.11 |
| 13. | $^{249}$Bk | $^{116}$Pd + $^{133}$Sb | $R_t$ | -0.63 | 36.83 | 16.82 | 16.78 |
| 14. | $^{249}$Cf | $^{121}$Cd + $^{128}$Sn | $R_t$ | -0.67 | 36.50 | 18.43 | 18.34 |
| 15. | $^{250}$Cf | $^{120}$Cd + $^{130}$Sn | $R_t$ | -0.35 | 32.42 | 11.57 | 11.71 |
| 16. | $^{253}$Es | $^{125}$In + $^{128}$Sn | $R_t$ | -0.80 | 32.84 | 13.26 | 13.30 |
| 17. | $^{250}$Fm | $^{124}$Sn + $^{126}$Sn | $R_t$ | -0.25 | 27.44 | 7.38 | 7.41 |
| 18. | $^{252}$Fm | $^{126}$Sn + $^{126}$Sn | $R_t$ | -0.55 | 32.66 | 9.62 | 9.60 |
| 19. | $^{254}$Fm | $^{126}$Sn + $^{128}$Sn | $C_t$ | -0.70 | 34.82 | 5.58 | 7.27 |
| 20. | $^{256}$Fm | $^{128}$Sn + $^{128}$Sn | $C_t$ | -0.70 | 28.66 | 1.94 | 4.00 |
| 21. | $^{255}$Md | $^{126}$Sn + $^{129}$Sb | $C_t$ | -0.66 | 33.98 | 5.10 | 6.04 |
| 22. | $^{257}$Md | $^{126}$Sn + $^{131}$Sb | $C_t$ | -0.65 | 30.30 | 1.97 | 6.30 |
| 23. | $^{259}$Md | $^{128}$Sn + $^{131}$Sb | $C_t$ | -0.65 | 25.97 | -1.41 | 3.76 |
| 24. | $^{256}$No | $^{124}$Sn + $^{132}$Te | $C_t$ | -0.44 | 24.88 | 2.12 | 2.04 |
| 25. | $^{257}$No | $^{125}$Sn + $^{132}$Te | $C_t$ | -0.51 | 27.05 | 3.21 | 3.23 |
| 26. | $^{259}$No | $^{126}$Sn + $^{133}$Te | $C_t$ | -0.60 | 28.29 | 0.68 | 4.54 |
| 27. | $^{252}$Lr | $^{120}$Sn + $^{132}$I | $R_t$ | 0.21 | - | 1.54 | 1.55 |
| 28. | $^{255}$Lr | $^{122}$Sn + $^{133}$I | $R_t$ | -0.28 | 22.06 | 4.08 | 4.34 |
| 29. | $^{256}$Lr | $^{120}$In + $^{136}$Xe | $R_t$ | -0.211 | - | 5.55 | 3.51 |
| 30. | $^{257}$Lr | $^{124}$Sn + $^{133}$I | $C_t$ | -0.55 | 26.50 | 3.05 | 3.34 |
| 31. | $^{259}$Lr | $^{129}$Sb + $^{130}$Te | $C_t$ | -0.55 | - | 0.594 | 3.76 |
| 32. | $^{256}$Rf | $^{122}$Sn + $^{134}$Xe | $R_t$ | 0.18 | 13.92 | -2.80 | -2.19 |
| 33. | $^{258}$Rf | $^{124}$Sn + $^{134}$Xe | $C_t$ | -0.108 | 18.34 | -1.82 | -1.85 |
| 34. | $^{259}$Rf | $^{124}$Sn + $^{135}$Te | $C_t$ | -0.45 | 23.66 | 1.60 | 1.60 |
| 35. | $^{258}$Sg | $^{120}$Sn + $^{138}$Ba | $C_t$ | 0.00 | 14.11 | -2.18 | -2.28 |
| 36. | $^{260}$Sg | $^{122}$Sn + $^{138}$Ba | $C_t$ | -0.185 | 16.04 | -2.08 | -2.14 |
| 37. | $^{262}$Sg | $^{124}$Sn + $^{138}$Ba | $C_t$ | -0.31 | 17.53 | -2.78 | -2.15 |
| 38. | $^{264}$Hs | $^{126}$Te + $^{138}$Ba | $C_t$ | -0.30 | 10.92 | -4.02 | -2.79 |

In table 2, the spontaneous fission half-lives of various parent nuclei particularly from $^{232}$U to $^{264}$Hs are tabulated. The calculations corresponding to inclusion of shell corrections are taken from [13]. In that study, the spontaneous fission half-lives are fitted using the neck-length, $\Delta$R in the presence of shell corrections and are found to be in agreement with the corresponding experimental data. Here, an effort is made to analyze the influence of excluding shell corrections on the half-lives. From the table, it is observed that for all the considered parent nuclei $^{232}$U to $^{264}$Hs, the spontaneous fission half lives increases in the absence of shell correction energy and far from agreement with the experimental data. It can be concluded that net effect of shell correction energy on the spontaneous fission half-lives is found to be negative.

It is also clear from Table 2, as the shell corrections are switched off, the atomic no.s of some of the experimentally observed clusters cannot be calculated.

Also, it is to be noted here that the shell effect for different possible decaying modes can be negative or positive but still the shell effect has negative effect on $T_{1/2.}$

## *Conclusion*

Presently, our main motive is to study the shell correction effect on the decay profile and spontaneous fission half life times of various parent nuclei particularly $^{232}$U to $^{264}$Hs using the Preformed Cluster-decay Model (PCM) which employs quantum mechanical fragmentation theory (QMFT) as its main tool. In the present work, the spontaneous fission half lives are calculated in the absence of shell correction energy (δU) by taking the neck length from [13], obtained there by fitting the actual experimental half lives. The half life times with and without shell correction energy are compared. It is observed that half life times increase when we do not incorporate the shell corrections. The probability of preformation of daughter fragments along with maximum number of other fragments decreases when we switch off the shell corrections. Although, the positive as well as negative effects have been seen in the fragmentation profile and preformation probability, but the net effect reflected on the half lives is negative. The fragment shift has also been observed in some cases i.e. the atomic number of the fragments changes after excluding the shell correction energy and magicity of some nuclei also vanishes when shell correction energy is made zero.

## *References*


[1] B. M. Peake Journal of Chemical Education **66**, 738 (1989).

[2] E. Rutherford, Philosophical Magazine **21**, 669 (1911).

[3] W. V. Mayneord, Rep. Prog. Phys.**14**, 366 (1951).

[4] S. Fritzler, V. Malka, G. Grillon, J. P. Rousseau, F. Burgy, Applied Physics Letters **83**, 3039 (2003).

[5] V. M. Strutinsky, Nucl. Phys. A **95**, 420 (1967).

[6] W. D. Myers and W. J. Swiatecki, Nucl. Phys. **81**, 1 (1966).

[7] Z. Ge, C. Li, J. Li, G. Zhang, B. Li, X. Xu, Phys. Rev. C **98**, 034312 (2018).

[8] U. Mosel and W. Greiner, Z. Phys. **217**, 256 (1968).

[9] S.G. Nilson and C. F. Tsang, Nucl. Phys. A **131**, 1 (1969).

[10] V.Yu. Denisov, Phys. Rev. C **89**, 044604 (2014).

[11] K. Sharma, G. Sawhney, M. K. Sharma and R. K. Gupta, Eur. Phys. J. A **55**, 30 (2019).

[12] G Sawhney, K. Sandhu, M. K. Sharma, and R. K. Gupta, Eur. Phys. J. A **50**, 175 (2014).

[13] K. Sharma, G. Sawhney and M. K. Sharma, Phys. Rev. C **96**, 054307 (2017).

[14] R. Kumar, Phys. Rev. C **86**, 044612 (2012).

[15] R. Kumar and M. K. Sharma, Phys. Rev. C **85**, 054612 (2012).

[16] S. K. Arun and R. K. Gupta, Phys. Rev. C **79**, 064616 (2009).

[17] S. K. Arun, R. K. Gupta, S. Kanwar, B. B. Singh and M. K. Sharma, Phys. Rev. C **80**, 034317 (2009).

[18] A. Săndulescu, R. K. Gupta, W. Scheid, W. Greiner, Physics Letter B **60**, 225 (1976).

[19] S. S. Malik and R. K. Gupta Phys. Rev. C **39**, 5 (1989).

[20] W. Greiner and W. Scheid, J. Phys. G **12**, L229 (1986).

[21] N. K. Virk, M. K. Sharma, R. Kumar, Nucl. Phys A **981**, 89 (2019).